Glycobiology, 2018, vol. 28, no. 10, 802–812
doi: 10.1093/glycob/cwy063
Advance Access Publication Date: 27 July 2018
Original Article

Microbial Biology

EpsN from *Bacillus subtilis* 168 has UDP-2,6-dideoxy 2-acetamido 4-keto glucose aminotransferase activity in vitro

Chinmayi R Kaundinya[2], Handanahal S Savithri[3], K Krishnamurthy Rao[2,1], and Petety V Balaji[2,1]

[2]Department of Biosciences and Bioengineering, Indian Institute of Technology Bombay, Powai, Mumbai 400076, India and [3]Department of Biochemistry, Indian Institute of Science, CV Raman Road, Bengaluru 560012, India

[1]To whom correspondence should be addressed: Tel: +91-22-2576 7778; Fax: +91-22-2572 3480; e-mail: kkr@iitb.ac.in (K. K.R.); balaji@iitb.ac.in (P.V.B.)

Received 17 April 2018; Revised 29 June 2018; Editorial decision 2 July 2018; Accepted 4 July 2018

Abstract

The gene *epsN* of *Bacillus subtilis* 168 was cloned and overexpressed in *Escherichia coli*. Purified recombinant EpsN is shown to be a pyridoxal 5′-phosphate (PLP)-dependent aminotransferase by absorption spectroscopy, L-cycloserine inhibition and reverse phase HPLC studies. EpsN catalyzes the conversion of UDP-2,6-dideoxy 2-acetamido 4-keto glucose to UDP-2,6-dideoxy 2-acetamido 4-amino glucose. Lys190 was found by sequence comparison and site-directed mutagenesis to form Schiff base with PLP. Mutagenesis studies showed that, in addition to Lys190, Ser185, Glu164, Gly58 and Thr59 are essential for aminotransferase activity.

Key words: deoxyaminosugars, *eps* operon, nucleotide sugar pyridoxal 5′-phosphate dependent aminotransferase (SATs), *N,N′*-diacetylbacillosamine biosynthetic pathway enzyme.

Introduction

Bacillus subtilis 168 is a Gram-positive bacterium and a widely studied model organism. Several aspects of this organism have been extensively investigated e.g., DNA replication, repair and cell division, transcription, translation, motility and biofilm formation (Graumann 2017). Formation, regulation and functions of biofilm are not completely understood in this bacterium. Exopolysaccharide substances (EPSs) are the major constituents of biofilm. Polysaccharide components of EPS are abundant and are present outside the cell wall covalently bound to the cohesive layer or completely excreted outside (Hussain et al. 2017).

At least four types of EPS are known to be synthesized by *B. subtilis* (Nwodo et al. 2012). These four types differ from each other in their chemical composition and structural architecture and have been attributed with different functions (Nwodo et al. 2012). One of the types, known as structural EPS, is involved in water retention and cell protection and consists of polysaccharides made of fructose, glucose, galactose, fucose, glucuronic acid, L-rhamnose, GalNAc and *N*-acetylglucosamine (GlcNAc). Prevalence of each of these monosaccharides depends on the integrity of the *eps* operon (Chai et al. 2012; Cairns et al. 2014). EPS synthesis in *B. subtilis* is under the control of *eps* and *tap*A operons (Vlamakis et al. 2013).

The genome of *B. subtilis* 168 has been completely sequenced (Kunst et al. 1997) and this has led to the identification of putative *eps* operon. According to the annotation in the genome database, this operon consists of 16 genes and proteins encoded in this operon have been electronically annotated to have activities related to the formation of biofilm (Supplementary data, Table SI). Disruption and complementation studies have shown that the region containing *epsHIJK* is responsible for the formation of poly-*N*-acetylglucosamine in the EPS matrix (Yakandawala et al. 2011). Disruption of *epsE* (Guttenplan et al. 2010), *epsG* (Branda et al. 2001) and *epsH* (Branda et al. 2001) affects pellicle formation and flat colony morphology. Point mutation in *eps*C gene of the *eps* operon leads to a decrease in EPS production (Vlamakis et al. 2013). There is no other experimental evidence on the biological functions of the individual genes or of the operon.

The gene *epsN* (or *yufE*) encodes the protein EpsN which is annotated as a putative pyridoxal phosphate-dependent aminotransferase (UniProt ID: Q795J3). EpsN is a sequence homolog of *Campylobacter jejuni* PglE, *Neisseria gonorrhoeae* PglC and *Acinetobacter baumanii* WeeJ, which are all pyridoxal 5′-phosphate (PLP)-dependent aminotransferases involved in the biosynthesis of *N*,*N*′-diacetylbacillosamine. In this study, EpsN was overexpressed in *Escherichia coli* with the objective of experimentally determining its molecular function in vitro. It was found that EpsN is indeed a PLP-dependent aminotransferase which converts UDP-2,6-dideoxy 2-acetamido 4-keto glucose to UDP-2,6-dideoxy 2-acetamido 4-amino glucose.

Results

Expression and purification of EpsN

Plasmid p34230 was transformed into *E. coli* BL21(DE3)pLysS. Protein expression was induced by the addition of IPTG and the glutathione S-transferase (GST)-EpsN fusion protein was purified by GST affinity chromatography (Supplementary data, Figure S1). PLP was added to all the buffers used for purification. The GST tag was removed by on-column thrombin digestion of the fusion protein. The eluted protein was dialyzed to remove unbound PLP. The protein was purified to near homogeneity (Figure 1A). A peak corresponding to molecular mass of 42.725 kDa was observed in MALDI-MS (Figure 1B); the calculated molecular mass is 42.790 kDa (ProtParam tool; www.expasy.ch). A low-intensity peak corresponding to molecular mass of 84.986 kDa was also observed suggesting the presence of a dimer (Figure 1B).

Probing the binding of PLP to EpsN by absorption spectroscopy

The ε-amino group of Lys forms a Schiff base linkage with the aldehyde group of PLP and this adduct is known as an internal aldimine. It has a characteristic absorption maximum in the range 400–430 nm. The absorption spectrum of EpsN shows a peak at 409 nm (Figure 2A). On addition of 0.4 mM sodium hydroxide, the protein was denatured and the free PLP was released. As expected, the absorbance maximum shifted to 388 nm (Figure 2A). The presence of PLP in the reaction mixture was confirmed by mass spectrometry which shows a peak corresponding to 246.01 Da (Figure 2B). From these studies, it was concluded that purified EpsN has bound PLP.

Effect of L-cycloserine on PLP binding

L-Cycloserine (LCS) is a cyclic analog of serine and a potent irreversible inhibitor of PLP-dependent enzymes (Soper and Manning 1981; Peisach et al. 1998). PLP forms an adduct with LCS by breaking the Schiff base with the active site Lys and the formation of such an adduct mimics the formation of pyridoxamine 5′-phosphate (PMP) intermediate (Peisach et al. 1998). Absorption spectrum in the wavelength range 300–500 nm was recorded by adding 5 mM LCS to EpsN (dialyzed in the absence of PLP) after 5, 10, 30, 60, 120, 180 and 240 min (Figure 3A). The intensity of the peak at 409 nm decreased with time and concurrently new peaks appeared at 330 and 373 nm. As mentioned earlier, the 409 nm peak is a characteristic of the internal aldimine. The appearance of the 330 nm peak is suggestive of the formation of the PLP–LCS adduct (Noland et al. 2002); the 373 nm peak is a characteristic of an oxime intermediate (Peisach et al. 1998). The LCS-treated EpsN was dialyzed separately in the presence/absence of PLP (Figure 3B). The 409 nm peak is observed only in the sample dialyzed against the PLP-containing buffer indicating that PLP replaces the PLP–LCS adduct. This observation confirms that purified EpsN has bound PLP.

Formation of Schiff base with active site lysine

The covalent bond between the ε-amino group of lysine and aldehyde group of PLP in PLP-containing proteins can be reduced by sodium cyanoborohydride ($NaCNBH_4$) (Hughes et al. 1962). The

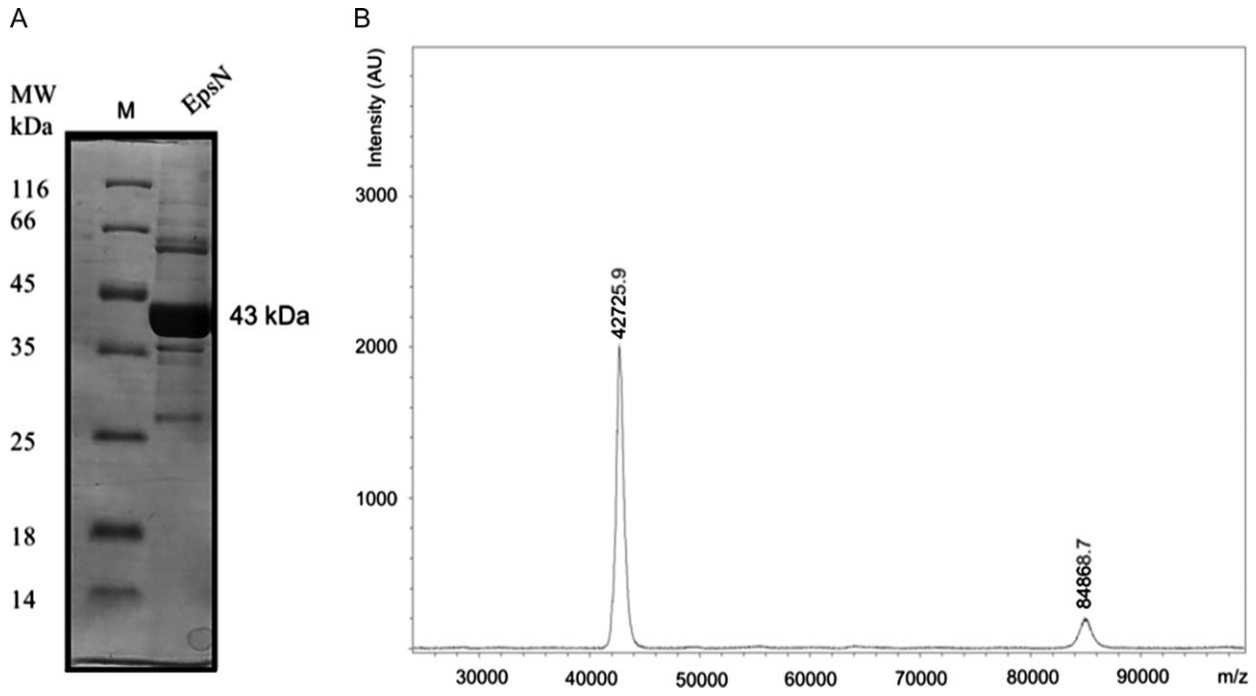

Figure 1. Purification of EpsN. (**A**) 12% SDS-PAGE of the purified EpsN. (**B**) MALDI-MS of the purified EpsN.

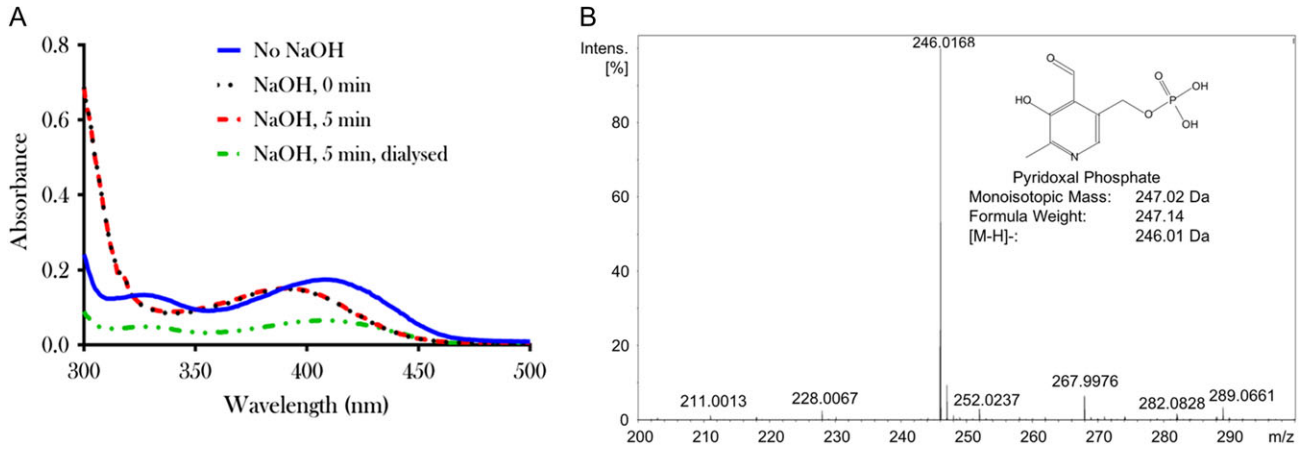

Figure 2. (**A**) Absorption spectra of purified EpsN before and after denaturation with NaOH. The absorption maxima are at 409 nm (before denaturation) and 388 nm (after denaturation). Spectrum recorded after dialyzing the denatured protein against a buffer containing PLP is also shown. (**B**) ESI-MS of denatured EpsN.

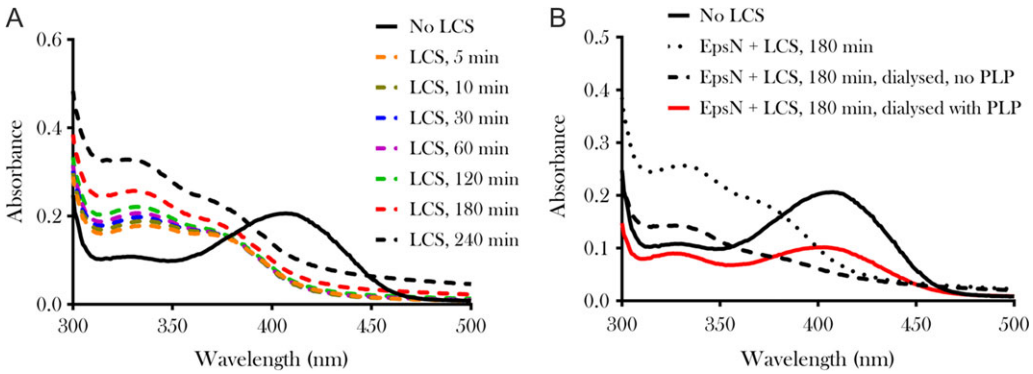

Figure 3. (**A**) Absorption spectra of EpsN treated with 5 mM L-cycloserine (LCS) acquired at different time points. The absorption maximum is at 409 nm in the absence of LCS and absorption maxima are at 330 and 373 nm after incubating with LCS. (**B**) Absorption spectra of EpsN before and after treating with LCS and after dialyzing the LCS-treated protein in the absence and presence of PLP.

resultant secondary amine has a characteristic absorption maximum in the range 325–335 nm (Hughes et al. 1962; Simon 2009; Amidani et al. 2017). If indeed such a shift occurred, then it would be suggestive that a Schiff base was formed and reduced by cyanoborohydride. Purified EpsN was first dialyzed against a buffer that does not contain PLP. To this dialyzed sample, 0.5 mM of $NaCNBH_4$ was added and absorption spectrum in the wavelength range 300–500 nm was recorded at 0, 5, 10, 30, 60, 120, 180 and 240 min (Figure 4A). The absorption maximum shifts from 409 to 329 nm (Figure 4A). A single peak at 329 nm is observed for EpsN treated with $NaCNBH_4$ for 240 min and then dialyzed in the absence of PLP (Figure 4B) showing that PLP bound to EpsN through a Schiff base is reduced to a secondary amine by the added $NaCNBH_4$.

Assay for in vitro aminotransferase activity by absorption spectroscopy

A comparison of the absorption spectra of EpsN before and after the addition of L-glutamate shows that the absorption maximum shifts from 409 to 327 nm in the presence of L-glutamate (Figure 5A) indicating the formation of PMP. The absorption maximum shifts back to 409 nm upon addition of UDP-keto sugar (Figure 5A), the acceptor substrate. The amino group gets transferred from PMP to UDP-keto sugar, regenerating PLP. The 409 nm peak is not restored when uridine 5′-diphosphate-*N*-acetylglucosamine (UDP-GlcNAc) was used as the acceptor substrate (Figure 5B). This observation suggests that EpsN exhibits aminotransferase activity in vitro with UDP-keto sugar as the substrate but not with UDP-GlcNAc. The aminotransferase activity was also assayed using different amino acids as the amino group donor; the activity is highest with L-glutamate and much lesser with L-glutamine and L-aspartate (data not shown).

Assay for in vitro aminotransferase activity by reverse phase HPLC

To further support the observation that EpsN has aminotransferase activity, the product formed was identified by reverse phase HPLC. For this, EpsN was incubated with L-glutamate and UDP-keto sugar for 150 min and the reaction was stopped by heating at 95°C for 10 min. The sample was injected on to a reverse phase HPLC column and the eluting species were monitored at 262 nm. The peaks at retention times of 16.7 and 25 min are from the reaction components (these peaks have not been assigned any number). Peak 2 at retention time of 17–17.8 min corresponds to UDP-keto sugar

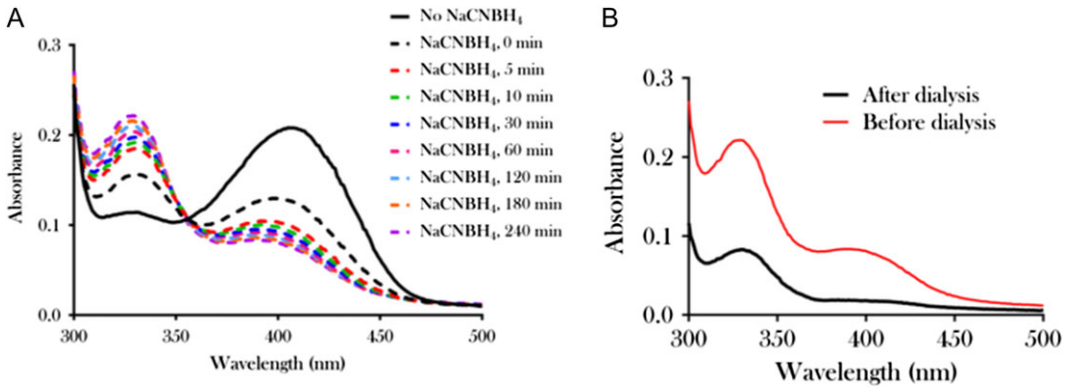

Figure 4. (**A**) Absorption spectra of EpsN treated with $NaCNBH_4$ for different durations. The absorption maximum shifts from 409 to 329 nm. (**B**) EpsN was treated with $NaCNBH_4$ for 240 min and dialyzed against a buffer that does not contain PLP. Absorption spectra were recorded before and after dialysis.

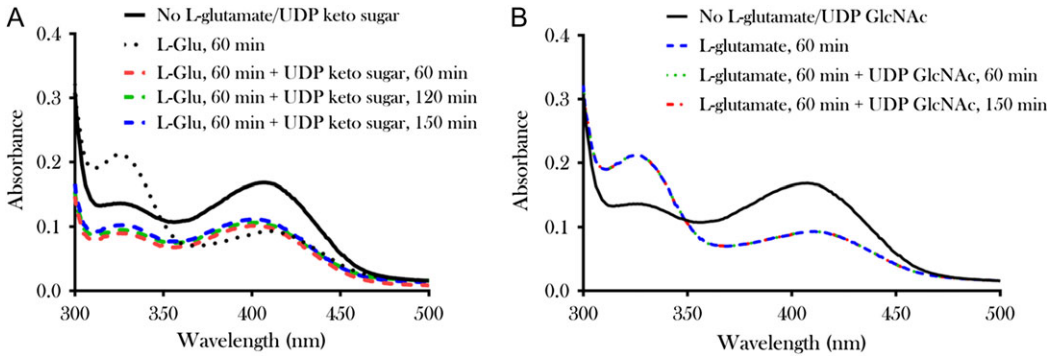

Figure 5. (**A**) Absorption spectra of EpsN before and after the addition of L-glutamate and UDP-keto sugar (UDP-keto sugar was obtained as described in Material and methods section and used immediately). The absorption maximum shifts from 409 to 327 nm in the presence of L-glutamate and absence of UDP-keto sugar indicating the formation of pyridoxamine 5′-phosphate. The absorption maximum shifts back to 409 nm in the presence of UDP-keto sugar, the acceptor substrate. (**B**) Absorption spectra of EpsN before and after the addition of L-glutamate and UDP-GlcNAc. The spectrum of the protein incubated with L-glutamate for 60 min remains the same even after the addition of UDP-GlcNAc.

(Figure 6B). Two new peaks were observed corresponding to retention times 14.0–14.4 min (peak 1) and 28.1–28.6 min (peak 3) and intensities of these two peaks increased with time (Figure 6A). Peak fractions were subjected to ESI-MS. The molecular mass of peak 1 fraction was 588.09 Da (Figure 6C) indicating the formation of UDP 2,6-dideoxy 2-acetamido 4-amino sugar (UDP-amino sugar). The molecular mass of peak 3 fraction is 246.01 Da which corresponds to PLP (data not shown). These observations confirm that EpsN indeed has UDP-keto sugar aminotransferase activity in vitro. For EpsN, K_m for UDP-keto sugar and V_{max} were calculated to be 387.5 μM and 3 μM/min, respectively.

Identifying the PLP-binding pocket in EpsN by homology modeling

The 3D structure of EpsN was modeled using the 3D structures of *Caulobacter crescentus* GDP-perosamine synthase, *Helicobacter pylori* PseC, *Pseudomonas aeruginosa* WbpE and putative UDP-4-amino-4-deoxy-l-arabinose-oxoglutarate aminotransferase from *Burkholderia cenocepacia* as templates. All these are aminotransferases that use a sugar nucleotide as a substrate. The top model was superimposed on the 3D structure of PLP-bound PglE (PDB ID 1O61). Gly58, Thr59, Asp161, Gln164, Ser185 and Lys190 were found to be within 4 Å from PLP.

Site-directed mutagenesis of PLP-binding pocket residues

All the five residues identified as above to be in the vicinity of PLP were mutated singly to Ala, Asp or Gln to study the effect on in vitro aminotransferase activity. The T59-OH group is in the proximity of the phosphate group of PLP and the S185-OH group is in the proximity of the OH group of ribose as well as the phosphate group. These interactions are expected to be disrupted in T59A, S185A and S185D mutants. The side chain carboxylate group of E164 interacts with the OH group of the pyridoxal ring and this interaction is expected to be weakened/eliminated in the E164D and E164A mutants. In addition to these single-residue mutants, G58 was also mutated to alanine, the corresponding residue in *C. jejuni* PglE (alignment position 76; Supplementary data, Figure S4), and K190 was mutated to either alanine or glutamine. The mutant proteins were overexpressed and purified similar to the wild-type protein (Supplementary data, Figure S2).

Secondary structure and oligomeric state of wild-type and mutant EpsN

Far UV circular dichroism (CD) spectrum of EpsN exhibits two troughs, at 209 and 222 nm (Figure 7), a characteristic of globular proteins with significant helical content. The secondary structure is not affected by any of the mutations (Figure 7). The mutants were also found to be homodimers (Supplementary data, Figure S3). However, one or more additional

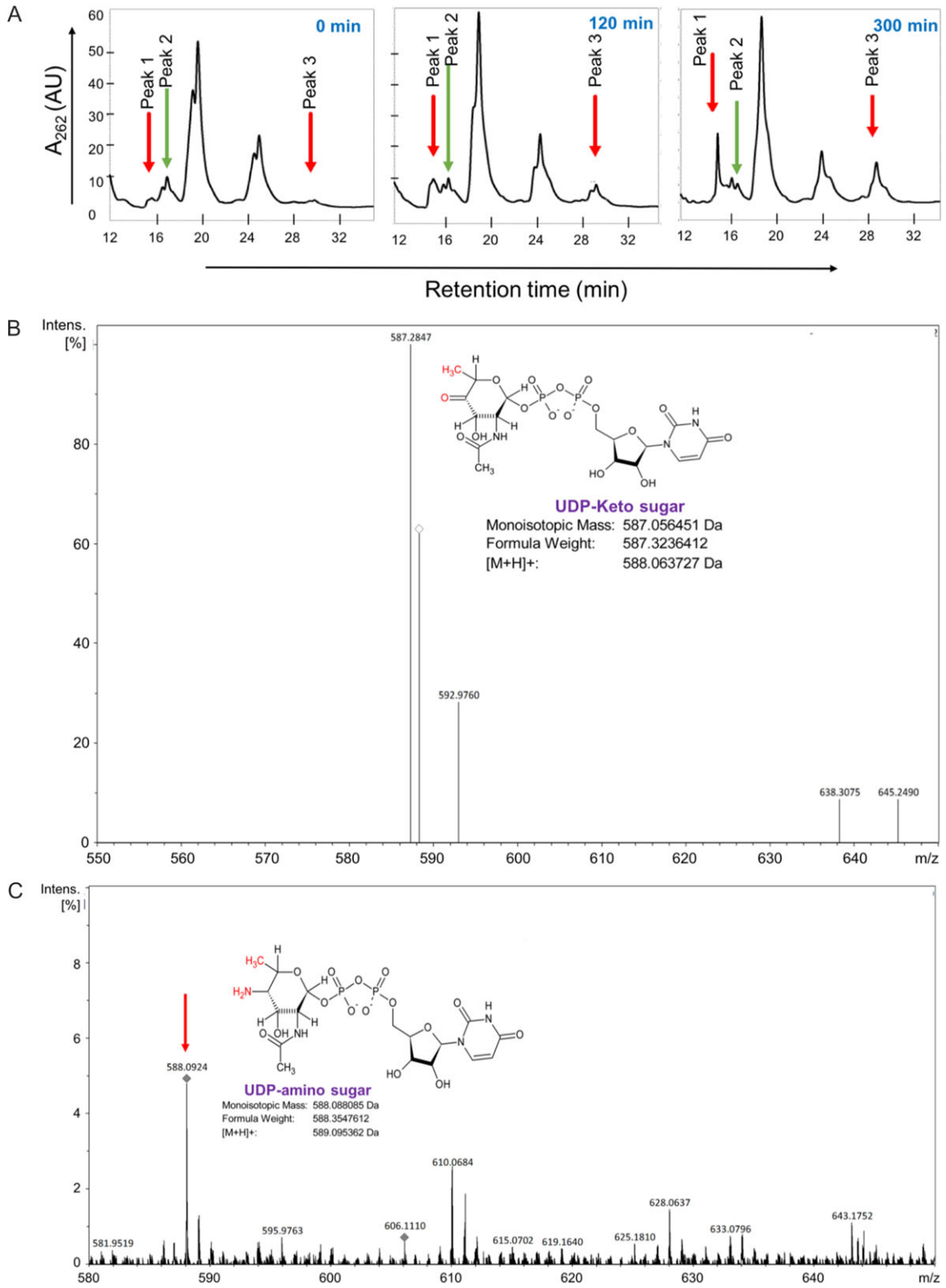

Figure 6. (**A**) Reverse phase HPLC time course profiles of the reaction mixture for the enzyme activity assay of EpsN at 0, 120 and 300 min, respectively. Three peaks are marked: peak 1 at 14.0–14.4 min, peak 2 at 17.0–17.8 min and peak 3 at 28.1–28.6 min. Peak 2 corresponds to UDP-keto sugar. (**B**) ESI-MS of peak 2 fraction. (**C**) ESI-MS peak 1 fraction.

peaks are observed for K190A, K190Q, S185D, S185A, G58A and T59A mutants; intensities and elution volumes of these additional peaks vary. A significantly larger fraction exists as higher oligomers in the case of T59A (~half) and G58A (~two-thirds) unlike in the case of other mutants. By comparison with PseC which also is a dimer (Schoenhofen et al. 2006a), G58 and T59 may be inferred to be in the dimer interface.

Effect of mutation on PLP binding and activity

In the case of K190A and K190Q mutants, (i) the 409 nm peak characteristic of Schiff base is absent in the absorption spectra and (ii) there is no change in absorption spectra upon the addition of L-glutamate (Figure 8). These two mutants are inactive (Figure 9) and the secondary structure content is same as that of the wild type (Figure 7). This lysine is conserved (alignment position 223) in other PLP-dependent enzymes that transfer amino group to UDP-keto sugar or its analogs (Supplementary data, Figure S4). Lys190 of EpsN corresponds to this conserved lysine. It can be inferred from these results and observations that PLP forms Schiff base with Lys190.

The absorption maximum is at 409 nm in the case of S185A and S185D mutants (Figure 8) suggesting that PLP has formed Schiff base in these two mutants. Upon addition of L-glutamate, absorption maximum does not shift from 409 to 327 nm (Figure 8) suggesting that PMP could not be formed. Expectedly, both mutants have lost aminotransferase activity as determined by reverse phase HPLC (Figure 9). The secondary structure content and oligomeric states of both the mutants are same as those of the wild type suggesting that S185 is functionally important.

The E164D mutant possess ~7-fold lesser activity when compared to wild-type EpsN and E164A mutant has lost activity (Figure 9). PLP forms a Schiff base in the E164D mutant (absorption maximum is at 409 nm) and PLP gets converted to PMP upon the addition of L-glutamate (absorption maximum shifts from 409 to 327 nm; Figure 8). The decrease in the intensity of the 409 nm peak suggests a change in the microenvironment of PLP in E164 mutant. The 409 nm peak in the absorption spectrum of the E164A mutant is barely visible and there is no shift in the absorption maximum when L-glutamate is added (Figure 8).

The 409 nm peak characteristic of Schiff base is absent in the absorption spectra of G58A and T59A mutants (Figure 8). Consistent with this, no change is observed in the absorption spectra upon the addition of L-glutamate (Figure 8) and neither of the two mutants exhibit aminotransferase activity (Figure 9). The loss of activity in these mutants is due to the absence of PLP at the active site which confirms the role of G58 and T59 in PLP binding.

Discussion

EpsN (UniProt id Q795J3) is encoded by the gene *epsN* of *B. subtilis* 168 and has been annotated as a putative aminotransferase involved in polysaccharide biosynthesis in the UniProt database. In this study, EpsN was overexpressed and the purified protein was shown by reverse phase HPLC to catalyze the transfer of amino group from L-glutamate to UDP-4-keto-2,6-dideoxy-2-acetamido glucose (Figure 6A). Further, the enzyme was shown to be PLP-dependent by (i) absorption spectroscopy (Figures 2 and 4) and (ii) reconstitution of the holoenzyme by adding free PLP to the apo enzyme, which in turn was obtained by treatment with LCS (Figure 3). Thus, EpsN is homologous to fold type I PLP-dependent aminotransferases that utilize sugar nucleotides as substrates. Site-directed mutagenesis studies have shown that Lys190, Ser185, Glu164, Thr59 and Gly58 are essential for activity. Mutation of Lys190 takes away the ε amino group which is required by PLP to form Schiff base (Figure 8). Loss of activity upon mutation of active site lysine has been reported in other sugar nucleotide aminotransferases, e.g., GDP-perosamine synthase (Cook and Holden 2008), PglE (Riegert et al. 2015), WbpE (Larkin et al. 2010) and WlaRG (Dow et al. 2017). Ser185 is also conserved like Lys190 (Supplementary data, Figure S4). In the Ser185 mutant, PLP forms the Schiff base as Lys190 is intact; however, the mutants fail to form the external aldimine and PMP (Figure 8). Glu164, Thr59 and Gly58 mutants are inactive because they do not bind PLP (Figure 8). In this study, Lys190, Ser185, Glu164, Thr59 and Gly58 have been shown to be crucial for PLP binding and hence the activity of the enzyme. Comparative modeling studies show that these residues are in the PLP binding pocket. Sequence comparison studies have shown that EpsN is a sequence homolog of *C. jejuni* PglE, *N. gonorrhoeae* PglC and *A. baumanii* WeeJ (Supplementary data, Table SII) which are aminotransferases involved in the biosynthesis of *N*, *N*′-diacetylbacillosamine (Olivier et al. 2006; Hartley et al. 2012; Morrison and Imperiali 2013).

N,*N*′-diacetylbacillosamine is 2,4-diacetamido-2,4,6-trideoxy-D-glucose and has been found only in prokaryotes to date. This monosaccharide was first identified in *Bacillus licheniformis* (Sharon 2007) but the pathway for its biosynthesis has so far been reported in bacteria of other genera, that is, *C. jejuni* (Olivier et al. 2006), *N. gonorrhoeae* (Hartley et al. 2012) and *A. baumanii* (Morrison and Imperiali 2013). This biosynthetic pathway involves dehydratase, aminotransferase and acetyltransferase. From *Bacillus* genus, five dehydratases, two aminotransferases and one acetyltransferase have been reported (Supplementary data, Table SIII). *Bacillus thuringiensis* Pam uses UDP-4-keto-6-deoxy-L-AltNAc which differs from UDP-4-keto-6-deoxy-D-GlcNAc (substrate used by EpsN) in the configuration of C5 carbon. In contrast, *Bacillus cereus* Pat uses the same substrate as EpsN. However, pair-wise sequence comparisons show that EpsN is more similar to *B. thuringiensis* Pam (UniProt id Q3ESA3, 50% similarity and 8% gaps) than to *B. cereus* Pat (Q814Z4, 45% similarity and 13% gaps).

Several PLP-dependent fold type I aminotransferases that utilize a sugar nucleotide as a substrate have been characterized experimentally and 3D structures have also been determined for some of them (Supplementary data, Table SIV). From the view point of the reaction catalyzed, these enzymes differ from each other as follows: (i) The keto group in the substrate is either at C-3 or C-4 carbon. (ii) The amino group is added in either equatorial or axial orientation. (iii) The nucleotide is UDP, GDP, TDP or dTDP. (iv) The sugar is glucose, GlcNAc or mannose. Structurally, they all are functional dimers (Schoenhofen, et al. 2006b; Burgie et al. 2007; Thoden et al. 2009; Larkin et al. 2010; van Straaten et al. 2013; Riegert et al. 2015; Wang et al. 2015; Dow et al. 2017) with each monomer consisting of two CATH domains (Sillitoe et al. 2015). Each of the two active sites is located at a dimer interface. Sequence divergence of these homologs (26–76% pair-wise sequence similarity) has resulted in substrate/product differences (Supplementary data, Table SV). In the PLP-binding pocket, a Lys (for Schiff base formation) and an

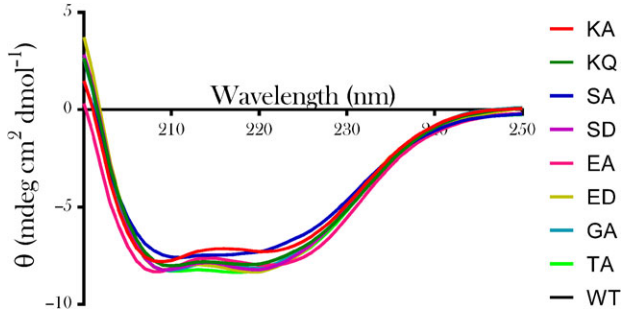

Figure 7. Far UV circular dichroism (CD) spectra of wild-type and mutant EpsN. All the proteins exhibit troughs at 209 and 222 nm.

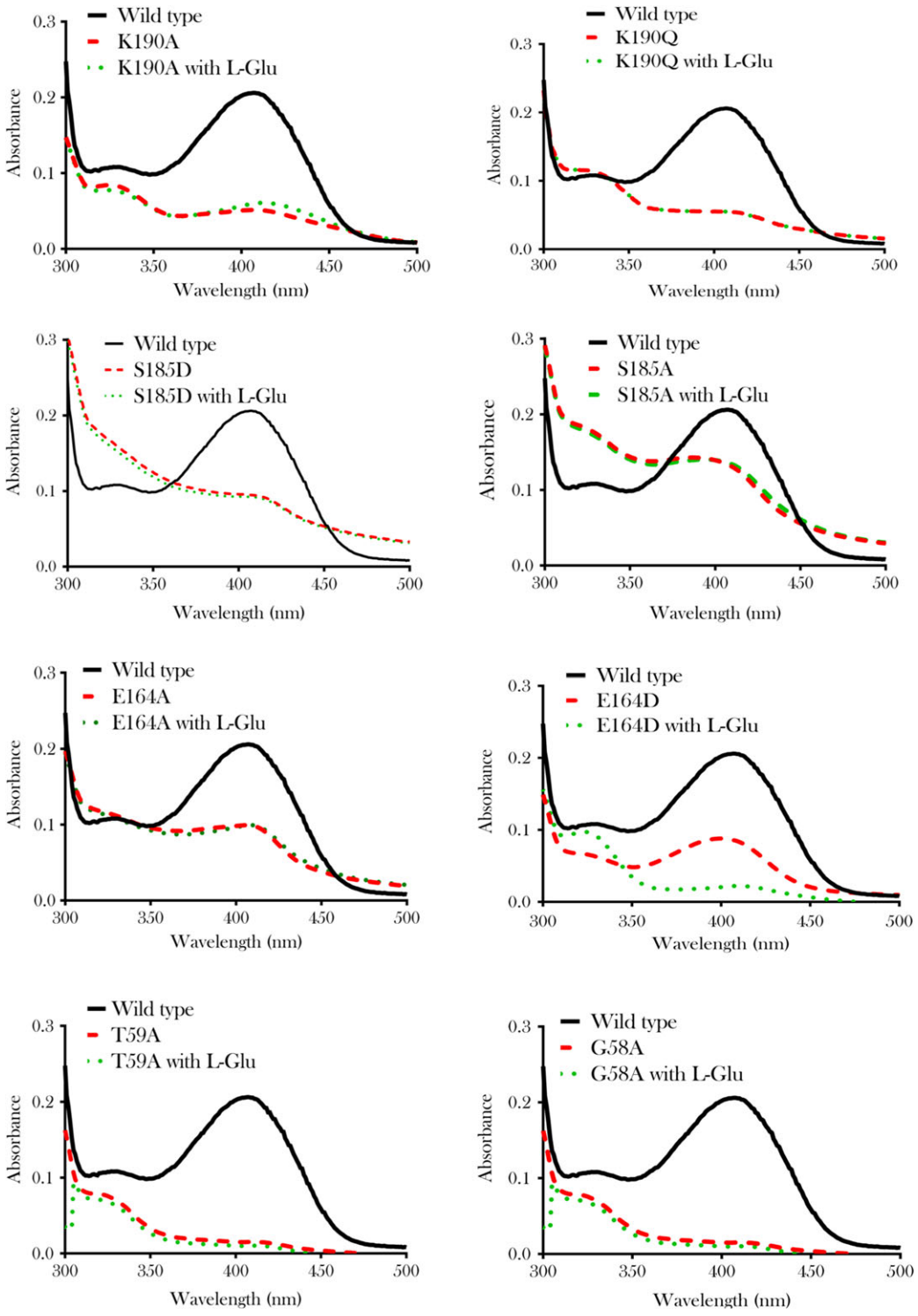

Figure 8. Absorption spectra of EpsN mutants in the absence (dotted line) and presence (solid line) of L-glutamate. The spectrum for the wild-type EpsN in the absence of L-glutamate (solid black line) is also shown in all the panels.

Asp [acts as the general acid (Wang et al. 2015)] are among the residues that are absolutely conserved (Lys190 and Asp161 in EpsN) (Supplementary data, Figure S4). Most of the protein–sugar interactions are water mediated (Vijayakumar et al. 2006; Thoden et al. 2009; Riegert et al. 2015) and sequence conservation is found only among proteins which use C-3 or C-4 keto substrate. Among the eight aminotransferases which use a C-4 keto substrate, EpsN is closest to *C. jejuni* PglE: sequence similarity 62% overall and 90% at the active site (Supplementary data, Table SV).

EpsN is a member of *eps* operon from *B. subtilis* 168. The *eps* operon contributes to exopolysaccharide biosynthesis along with other genes and operons. The other members of the *eps* operon have

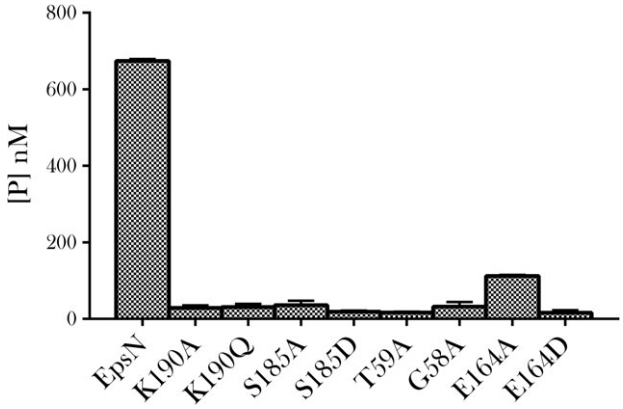

Figure 9. Reverse phase HPLC-based assay for aminotransferase activity of wild-type and mutant EpsN.

been annotated to be involved in sugar biosynthesis (Supplementary data, Table SI). EpsC and EpsM are sequence homologs of dehydratase and acetyltransferase, respectively, involved in the biosynthesis of *N*,*N*′-diacetylbacillosamine in *C. jejuni*, *N. gonorrhoeae* and *A. baumanii* (Supplementary data, Table SII). If similarity in sequence translates to similarity in enzyme activities, then EpsC and EpsM will have dehydratase and acetyltransferase activities, respectively. As mentioned earlier, EpsN is a sequence homolog of the aminotransferases in these three organisms. Based on these, it is hypothesized that EpsC, EpsN and EpsM are together involved in the biosynthesis of *N*,*N*′-diacetylbacillosamine and that is used as a building block in the biosynthesis of EPS. In *C. jejuni*, PglE knockout mutants could not colonize or cause virulence in the host because of impaired flagellar-mediated motility and PglE is required for protein glycosylation (Vijayakumar et al. 2006). Phenotypic consequence of knocking out genes that encode enzymes of the *N*,*N*′-diacetylbacillosaminebiosynthesis have not been investigated in either *N. gonorrhoeae* or *A. baumanii*.

The expression levels of the *eps* operon has been proposed to control the switch from motility to biofilm to sporulation (Cairns et al. 2014). EPS is synthesized under varied environmental conditions viz., the presence of excess carbon source concomitantly limited by another nutrient (e.g., nitrogen or oxygen) or under aerobic conditions (Freitas et al. 2011). The *eps* operon is regulated by a spectrum of transcriptional regulators viz., cis-acting RNA element called eps-associated RNA and transcription repressors AbrB, SinR, RemA and RemB (Cairns et al. 2014). Expression of *eps* operon is also controlled by Sigma-H, an alternate sigma factor (Britton et al. 2002). The *eps* operon is also under the control of quorum-sensing elements like "LuxS by Autoinducer-2" (AI-2; lactose induced) (Longwell and Dube 2013) and ComA of the ComX-ComP-ComA pathway (Comella and Grossman 2005); this pathway directly regulates swarming motility and surfactin production in *B. subtilis* and indirectly regulates biofilm formation (Comella and Grossman 2005). Experimental characterization of the molecular functions of *eps* operon genes is essential to completely understand the biological role of this operon.

Materials and methods

Materials

β-Nicotinamide adenine dinucleotide (NAD^+) sodium salt, L-glutathione (oxidized and reduced), $NaCNBH_4$, LCS and UDP-GlcNAc were from Sigma Aldrich, St. Louis, MO. Plasmids and *E. coli* strains were from laboratory stocks. All other reagents and chemicals were of analytical grade.

Cloning of EpsN

The gene encoding EpsN was PCR amplified using gene-specific primers (Table I), genomic DNA from *B. subtilis* 168 and Phusion® polymerase (Finzymes). PCR amplifications were performed in total volume of 50 µL containing 1X PCR buffer, 2.5 mM dNTP (Thermo Fisher Scientific), 100 nM each of forward and reverse primers (Sigma Aldrich, India), 50 ng template DNA (Genomic DNA isolation kit from Promega) and 0.5 units of Phusion® polymerase under the conditions of denaturation at 94°C, 1 min, annealing at 45°C (first 5 cycles) or 62°C (next 35 cycles) and extension at 72°C, 150 s. Initial denaturation was for 5 min. The amplified product was cloned into the pGEX-4T-1 vector at BamHI and XhoI sites and the resultant plasmid was named as p34230. This plasmid was sequenced (Macrogen, South Korea) to ensure the identity of the gene. Restriction digestion and ligation were carried out according to the manufacturers' protocol. The protein will be expressed as a fusion protein with N-terminal GST tag.

Site-directed mutagenesis

Point mutations were introduced following the PCR-based site-directed mutagenesis method described by Weiner and Costa (1994). PCR reactions were carried out using p34230 as the template, appropriate primers (Table I) and Phusion® polymerase. PCR amplifications were performed as described earlier and the PCR products were digested with DpnI at 37°C for 8 h to remove the template DNA. Plasmids were purified following standard protocol (Green and Sambrook 2012) and screened by digestion with appropriate restriction enzymes. Mutations were confirmed by sequencing (Macrogen, South Korea).

Expression and purification of recombinant proteins

Competent *E. coli* cells were prepared following calcium chloride and manganese chloride method (Green and Sambrook 2012). The plasmid p34230 was transformed into BL21(DE3)pLysS competent cells, plated onto an LB agar plate containing 50 µg/mL ampicillin and incubated at 37°C for 12 h. A single colony was inoculated into 50 mL LB medium containing 50 µg/mL ampicillin and incubated for 12 h at 37°C with constant shaking at 180 rpm. Preinoculum was inoculated into LB medium in 1:100 ratio containing 50 µg/mL ampicillin and grown at 37°C with constant shaking at 180 rpm till OD_{600} reached 0.8 (~3.5 h). Protein expression was induced by adding IPTG to a final concentration of 1 mM and incubating for 6 h at 30°C with constant shaking at 80 rpm. Cells were harvested at 11,305 × *g* for 10 min at 4°C. The pellet was resuspended in extraction buffer (phosphate-buffered saline buffer, pH 7.5 with 100 µM PLP (AMRESCO) and 5% glycerol) (approximately one-tenth the culture volume). Cells were sonicated for 15 min with intermittent cooling (3-s ON and 2-s OFF) and centrifuged at 20,216 × *g* for 15 min at 4°C to remove cell debris. The recombinant protein was purified from the supernatant using GST affinity chromatography (Novagen, Madison, WI). The slurry was incubated at 4°C for 3 h on an end-to-end rotor, loaded onto an empty column and the unbound fraction was allowed to pass through. The column was washed with two column volumes of extraction buffer. The N-terminal GST tag was removed by on-column digestion by adding

Table I. PCR primers used in this study

Primer[a]	Primer sequence (5′–3′)[b]	Restriction enzyme
CRK101FP	GGCCGGATCCATGCATAAAAAAATCTACTTATCTCCC	BamHI
BSU3423RP	ATATCTCGAGTCATCGAATGCTTGCTGTCCATTTC	XhoI
S185D FP	CGC TTC GGA ATA TTT GAC TTT AAC G	SspI
S185D RP	CC GTT AAA GTC AAA TAT TCC GAA GCG	SspI
S185A FP	CGC TTC GGA ATA TTT GCA TTT AAC GG	SspI
S185A RP	CC GTT AAA TGC AAA TAT TCC GAA GCG	SspI
G58A FP	GCG GTC GGA TCC GCA ACG GCG GCG	BamHI
G58A RP	CGC CGC CGT TGC GGA TCC GAC CGC	BamHI
T59A FP	GCG GTC GGA TCC GGA GCG GCG GCG	BamHI
T59A RP	CGC CGC CGC TCC GGA TCC GAC CGC	BamHI
E164A FP	C GCA GCC GCA TCT CTC GGT ACC GTC TAT	KpnI
E164A RP	ATA GAC GGT ACC GAG AGA TGC GGC TGC G	KpnI
E164D FP	C GCA GCC GAT TCT CTC GGT ACC GTC TAT	KpnI
E164D RP	ATA GAC GGT ACC GAG AGA ATC GGC TGC G	KpnI
K190A FP	C GGG AAC GCA ATC ATC ACC ACG TCA GG	BmgBI
K190A RP	CC TGA CGT GGT GAT GAT TGC GTT CCC G	BmgBI
K190Q FP	C GGG AAC CAA ATC ATC ACC ACG TCA GG	BmgBI
K190Q RP	CC TGA CGT GGT GAT GAT TTG GTT CCC G	BmgBI

[a]FP-Sense primer and RP-Antisense primer.

[b]Restriction enzyme sites are underlined. In primers used for site-directed mutagenesis, site of mutation is double underlined.

1 U thrombin (Novagen, Madison, WI) per milliliter of beads and incubated on an end-to-end rotor for 12 h at 22°C. The eluted protein was dialyzed against phosphate-buffered saline buffer, pH 7.5 containing 5% glycerol to remove excess PLP. Protein was concentrated using centrifugal filter units with 30 kDa MWCO (Merck-Millipore, Germany) and stored at 4°C until further use.

Substrate for aminotransferase activity

The substrate was generated enzymatically as follows: purified EpsC (unpublished data) was added to 5 mM oxidized L-glutathione, 50 mM Tris-acetate pH 8.0, 0.1% Triton X-100, 200 µM NAD^+, 50 mM NaCl, 200 µM UDP-GlcNAc incubated for 210 min at 37°C; the reaction mixture was fractionated on a HPLC column and the concentration of UDP 2,6-dideoxy 2-acetamindo 4-keto glucose was estimated to be 75 µM based on the area under the corresponding peak. This reaction mixture was heated at 95°C for 10 min, centrifuged briefly and the supernatant was used as the UDP 2,6-dideoxy 2-acetamindo 4-keto glucose solution to assay the aminotransferase activity of EpsN.

Assay for aminotransferase activity of EpsN

The reaction mixture consisted of 0–150 µM UDP 2,6-dideoxy 2-acetamindo 4-keto glucose, 23.4 µM EpsN, 15 µM L-glutamate. The reaction mixture was incubated at 28°C for 150 min and the reaction was monitored by absorption spectroscopy and reverse phase HPLC. For analysis by reverse phase HPLC, the reaction was stopped by heating at 95°C for 10 min followed by centrifugation at 20,216 × *g* for 10 min and the supernatant was injected onto the column.

Absorption spectroscopy

Absorption spectra of wild-type and mutant EpsN under different conditions in the range 300–500 nm were recorded at a scan speed of 100 nm/min in a JASCO UV-Visible V-530 spectrophotometer. 1 mg/mL of protein in phosphate-buffered saline buffer at pH 7.5 containing 5% glycerol was used.

Reverse phase HPLC

The aminotransferase assay mixture was analyzed by reverse phase HPLC as described previously (Rosazza 1998). HP Agilent 1100 HPLC system with binary pump and auto sampler (Agilent Technologies) and Ascentis® C18 HPLC Column (5 µm particle size, L × I.D. 25 cm × 4.6 mm) (Sigma Aldrich, St. Louis, MO) were used. Twenty microliters of sample were injected and separated using a gradient of buffer A (7.5 mM KH_2PO_4 pH 5.3, 5 mM tetra butyl ammonium hydroxide (TBAH) (Spectrochem, India) over buffer B (17.5 mM KH_2PO_4 pH 5.3, 5 mM TBAH and 30% acetonitrile) from 5% to 62% in 35 min at a flow rate of 1 mL/min. The eluting species were monitored at 262 nm.

ESI-MS of peak fractions of reverse phase HPLC

The aminotransferase assay mixture was analyzed by hydrophilic interaction chromatography (Hwang et al. 2014) by injecting 80 µL of sample onto an Accucore 150-amide HILIC column (150 × 4.6 mm, 2.6 m particle size, Thermo Fisher Scientific, Waltham, MA). Analytes were separated using 25% buffer A (40 mM of ammonium acetate, pH 4.35) and 75% buffer B (100% acetonitrile) for 2 min, a gradient of buffer A (25–65%) over buffer B (75–35%) from 2 to 23 min, a second gradient from 23 to 25 min (65–50% buffer A and 35–50% of buffer B) and from 25 to 35 min with equal amounts of buffer A and buffer B. The flow rate was set to 0.7 mL/min. The analytes were detected by MS (Impact HD ESI-QTOF, Bruker, Billerica, MA) detector with negative ion mode, detector voltage at 2000 V, end plate offset set at −500 V, capillary voltage at 3000 V and nebulizer at 2.0 Bar.

Size-exclusion chromatography

Size-exclusion chromatography of proteins was carried out in FPLC system AKTAPurifier (GE Healthcare Life Sciences, Chicago, IL) using a Superdex S-200 (GE Healthcare Life Sciences, Chicago, IL) (exclusion limit 600 kDa) prepacked column of preparative scale (bed volume 120 mL). The column was equilibrated with phosphate-buffered saline, pH 7.5 containing 5% glycerol at a flow rate of 0.5 mL/min.

1% of the bed volume of protein sample was loaded onto the column and eluted at a flow rate of 0.5 mL/min. The elution profile of the protein was monitored by measuring absorbance at 280, 215 and 260 nm (Triple UV channel).

CD spectroscopy

The secondary structure of the protein was determined by far-UV CD spectroscopy using a JASCO 815 spectropolarimeter with a scan speed of 100 nm/min at 25°C. The scan was acquired using 0.4 mg/mL of wild-type and mutant EpsN in a 0.1-cm path length cuvette. Protein concentrations were measured by Bradford method using BSA as the standard. The data from an average of three scans were used to plot spectra. The spectra of mutant proteins were normalized with respect to that of the wild type. The secondary structure content was calculated online by the K2D2 secondary structure prediction server (http://k2d2.ogic.ca/).

Homology modeling

The 3D structure of EpsN was modeled using the I-TASSER server with default values for all the parameters (Zhang 2008; Roy et al. 2010; Yang et al. 2015). Chimera (v1.12) was used for the superposition of 3D structures (Pettersen et al. 2004).

Supplementary data

Supplementary data are available at *Glycobiology* online.

Funding

This work was financially supported by a grant (2011/37B/43/BRNS with BSC) from the Board of Research in Nuclear Sciences (BRNS), Department of Atomic Energy, Government of India.

Acknowledgements

The authors thank Ms. Anu Prabha for her help with predicting PLP-binding residues and Prof. Suvarn Kulkarni and Prof. Dulal Panda for helpful discussions. CRK was supported by a Senior Research Fellowship under the INSPIRE program of the Department of Science and Technology, Government of India. The authors also thank Indian Institute of Technology Bombay and Indian Institute of Science for providing facilities and other infrastructure for carrying out this work.

Conflict of interest statement

None declared.

Abbreviations

PLP, pyridoxal 5′-phosphate; PMP, pyridoxamine 5′-phosphate; LCS, L-cycloserine; UDP-GlcNAc, uridine 5′-diphosphate-N-acetylglucosamine; UDP-keto sugar, uridine 5′-diphosphate-2,6-dideoxy 2-acetamido 4-keto glucose; UDP-amino sugar, uridine 5′-diphosphate-2,6-dideoxy 2-acetamido 4-amino glucose; GST, glutathione S-transferase; TBAH, tetrabutylammonium hydroxide; NAD^+, β-Nicotinamide adenine dinucleotide; $NaCNBH_4$, Sodium cyanoborohydride.

References

Amidani D, Tramonti A, Valeria A, Campanini B, Maggi S, Milano T, Martino L, Pascarella S, Contestabile R, Bettati S et al. 2017. Study of DNA binding and bending by *Bacillus subtilis* GabR, a PLP-dependent transcription factor. *Biochim Biophys Acta*. 1861:3474–3489.

Branda SS, González-Pastor JE, Ben-Yehuda S, Losick R, Kolter R. 2001. Fruiting body formation by *Bacillus subtilis*. *Proc Natl Acad Sci*. 98: 11621–11626.

Britton RA, Eichenberger P, Gonzalez-pastor JE, Fawcett P, Monson R, Losick R, Grossman AD, Acteriol JB. 2002. Genome-wide analysis of the stationary-phase sigma factor (sigma-H) regulon of *Bacillus subtilis*. *J Bacteriol*. 184:4881–4890.

Burgie ES, Thoden JB, Holden HM. 2007. Molecular architecture of DesV from *Streptomyces venezuelae*: A PLP-dependent transaminase involved in the biosynthesis of the unusual sugar desosamine. *Protein Sci*. 16:887–896.

Cairns LS, Hobley L, Stanley-wall NR. 2014. Biofilm formation by *Bacillus subtilis*: New insights into regulatory strategies and assembly mechanisms. *Mol Microbiol*. 93:587–598.

Chai Y, Beauregard PB, Vlamakis H, Losick R, Kolter R. 2012. Galactose metabolism plays a crucial role in biofilm formation by *Bacillus subtilis*. *MBio*. 3:1–10.

Comella N, Grossman AD. 2005. Conservation of genes and processes controlled by the quorum response in bacteria: Characterization of genes controlled by the quorum-sensing transcription factor ComA in *Bacillus subtilis*. *Mol Microbiol*. 57:1159–1174.

Cook PD, Holden HM. 2008. GDP-perosamine synthase: structural analysis and production of a novel trideoxysugar. *Biochemistry*. 47:2833–2840.

Dow GT, Gilbert M, Thoden JB, Holden HM. 2017. Structural investigation on WlaRG from *Campylobacter jejuni*: A sugar aminotransferase. *Protein Sci*. 26:586–599.

Freitas F, Alves VD, Reis MAM. 2011. Advances in bacterial exopolysaccharides: From production to biotechnological applications. *Trends Biotechnol*. 29:388–398.

Graumann PL. 2017. *Bacillus: Cellular and Molecular Biology*, 3rd ed. Norfolk, UK: Caister Academic Press.

Green MR, Sambrook J. 2012. *Molecular Cloning: A Laboratory Manual*, 4th ed. N.Y: Cold Spring Harbor Laboratory Press.

Guttenplan SB, Blair KM, Kearns DB. 2010. The EpsE flagellar clutch is bifunctional and synergizes with EPS biosynthesis to promote *Bacillus subtilis* biofilm formation. *PLoS Genet*. 6:e1001243.

Hartley MD, Morrison MJ, Aas FE, Børud B. 2012. Biochemical characterization of the O-linked glycosylation pathway in *Neisseria gonorrhoeae* responsible for biosynthesis of protein glycans containing N,N′-diacetylbacillosamine. *Biochemistry*. 50:4936–4948.

Hughes RC, Jenkins WT, Fischer EH. 1962. The site of binding of pyridoxal-5′-phosphate to heart glutamic-aspartic transaminase. *Proc Natl Acad Sci USA*. 48:1615–1618.

Hussain A, Zia KM, Tabasum S, Noreen A, Ali M, Iqbal R, Zuber M. 2017. Blends and composites of exopolysaccharides; properties and applications: A review. *Int J Biol Macromol*. 94:10–27.

Hwang S, Li Z, Bar-Peled Y, Aronov A, Ericson J, Bar-Peled M. 2014. The biosynthesis of UDP-d-FucNAc-4N-(2)-oxoglutarate (UDP-Yelosamine) in *Bacillus cereus* ATCC 14579: Pat and Pyl, an aminotransferase and an ATP-dependent Grasp protein that ligates 2-oxoglutarate to UDP-4-amino-sugars. *J Biol Chem*. 289:35620–35632.

Kunst F, Ogasawara N, Moszer I, Albertini AM, Alloni G, Azevedo V, Bertero MG, Bessières P, Bolotin A, Borchert S et al. 1997. The complete genome sequence of the Gram-positive bacterium *Bacillus subtilis*. *Nature*. 390:249.

Larkin A, Olivier NB, Imperiali B. 2010. Structural analysis of WbpE from *Pseudomonas aeruginosa* PAO1: A nucleotide sugar aminotransferase involved in O-antigen assembly. *Biochemistry*. 49:7227–7237.

Longwell SA, Dube DH. 2013. Deciphering the bacterial glycocode: Recent advances in bacterial glycoproteomics. *Curr Opin Chem Biol*. 17:41–48.

Morrison MJ, Imperiali B. 2013. Biosynthesis of UDP-N,N′-diacetylbacillosamine in *Acinetobacter baumannii*: Biochemical characterization and correlation to existing pathways. *Arch Biochem Biophys*. 536:72–80.

Noland BW, Newman JM, Hendle J, Badger J, Christopher J A., Tresser J, Buchanan MD, Wright T A., Rutter ME, Sanderson WE et al. 2002. Structural studies of *Salmonella typhimurium* ArnB (PmrH) aminotransferase. *Structure*. 10:1569–1580.

Nwodo UU, Green E, Okoh AI. 2012. Bacterial exopolysaccharides: Functionality and prospects. *Int J Mol Sci*. 13:14002–14015.

Olivier NB, Chen MM, Behr JR, Imperial B. 2006. In vitro biosynthesis of UDP-N,N′-diacetylbacillosamine by enzymes of the *Campylobacter jejuni* general protein glycosylation system. *Biochemistry*. 45:13659–13669.

Peisach D, Chipman DM, Van Ophem PW, Manning JM, Ringe D. 1998. D-cycloserine inactivation of D-amino acid aminotransferase leads to a stable noncovalent protein complex with an aromatic cycloserine-PLP derivative. *J Am Chem Soc*. 120:2268–2274.

Pettersen EF, Goddard TD, Huang CC, Couch GS, Greenblatt DM, Meng EC, Ferrin TE. 2004. UCSF Chimera-a visualization system for exploratory research and analysis. *J Comput Chem*. 25:1605–1612.

Riegert AS, Young NM, Watson DC, Thoden JB, Holden HM. 2015. Structure of the external aldimine form of PglE, an aminotransferase required for N,N'-diacetylbacillosamine biosynthesis. *Protein Sci*. 24:1609–1616.

Rosazza JPN. 1998. Enzymatic conversion of glucose to UDP-4-keto-6-deoxyglucose in *Streptomyces* spp. *Appl Environ Microbiol*. 64:3972–3976.

Roy A, Kucukural A, Zhang Y. 2010. I-TASSER: A unified platform for automated protein structure and function prediction. *Nat Protoc*. 5: 725–738.

Schoenhofen IC, Lunin VV, Julien JP, Li Y, Ajamian E, Matte A, Cygler M, Brisson JR, Aubry A, Logan SM et al. 2006a. Structural and functional characterization of PseC, an aminotransferase involved in the biosynthesis of pseudaminic acid, an essential flagellar modification in *Helicobacter pylori*. *J Biol Chem*. 281:8907–8916.

Schoenhofen IC, McNally DJ, Vinogradov E, Whitfield D, Young NM, Dick S, Wakarchuk WW, Brisson JR, Logan SM. 2006b. Functional characterization of dehydratase/aminotransferase pairs from *Helicobacter* and *Campylobacter*: Enzymes distinguishing the pseudaminic acid and bacillosamine biosynthetic pathways. *J Biol Chem*. 281:723–732.

Sharon N. 2007. Celebrating the golden anniversary of the discovery of bacillosamine, the diamino sugar of a *Bacillus*. *Glycobiology*. 17:1150–1155.

Sillitoe I, Lewis TE, Cuff A, Das S, Ashford P, Dawson NL, Furnham N, Laskowski RA, Lee D, Lees JG et al. 2015. CATH: Comprehensive structural and functional annotations for genome sequences. *Nucleic Acids Res*. 43:D376–D381.

Simon ES, Allison J. 2009. Determination of pyridoxal-5′-phosphate (PLP)-binding sites in proteins: A peptide mass fingerprinting approach based on diagnostic tandem mass spectral features of PLP-modified peptides. *Rapid Commun Mass Spectrom*. 23:3401–3408.

Soper TS, Manning M. 1981. Different modes of action of inhibitors of bacterial D-amino acid transaminase. *J Biol Chem*. 256:4263–4268.

Thoden JB, Schäffer C, Messner P, Holden HM. 2009. Structural analysis of QdtB, an aminotransferase required for the biosynthesis of dTDP-3-acetamido-3,6-dideoxy-α-D-glucose. *Biochemistry*. 48:1553–1561.

Van Straaten KE, Ko JB, Jagdhane R, Anjum S, Palmer DRJ, Sanders DAR. 2013. The structure of NtdA, a sugar aminotransferase involved in the kanosamine biosynthetic pathway in *Bacillus subtilis*, reveals a new subclass of aminotransferases. *J Biol Chem*. 288:34121–34130.

Vijayakumar S, Merkx-Jacques A, Ratnayake DB, Gryski I, Obhi RK, Houle S, Dozois CM, Creuzenet C. 2006. Cj1121c, a novel UDP-4-keto-6-deoxy-GlcNAc C-4 aminotransferase essential for protein glycosylation and virulence in *Campylobacter jejuni*. *J Biol Chem*. 281: 27733–27743.

Vlamakis H, Chai Y, Beauregard P, Losick R, Kolter R. 2013. Sticking together: Building a biofilm. *Nat Rev Microbiol*. 11:157–168.

Wang F, Singh S, Xu W, Helmich KE, Miller MD, Cao H, Bingman CA, Thorson JS, Phillips GN. 2015. Structural basis for the stereochemical control of amine installation in nucleotide sugar aminotransferases. *ACS Chem Biol*. 10:2048–2056.

Weiner MP, Costa GL. 1994. Rapid PCR site-directed mutagenesis. *Genome Res*. 4:S131–S136.

Yakandawala N, Gawande PV, LoVetri K, Cardona ST, Romeo T, Nitz M, Madhyastha S. 2011. Characterization of the poly-β-1,6-N-acetylglucosamine polysaccharide component of *Burkholderia* biofilms. *Appl Environ Microbiol*. 77:8303–8309.

Yang J, Yan R, Roy A, Xu D, Poisson J, Zhang Y. 2015. The I-TASSER Suite: Protein structure and function prediction. *Nat Methods*. 12:7–8.

Zhang Y. 2008. I-TASSER server for protein 3D structure prediction. *BMC Bioinformatics*. 8:1–8.